Computational investigation on the mechanism and the stereoselectivity of Morita–Baylis–Hillman reaction and the effect of the bifunctional catalyst *N*-methylprolinol†

Liang Dong, Song Qin, Zhishan Su, Huaqing Yang and Changwei Hu*

Received 6th April 2010, Accepted 15th June 2010
First published as an Advance Article on the web 9th July 2010
DOI: 10.1039/c004932h

The mechanism of the Morita–Baylis–Hillman (MBH) reaction between formaldehyde and methyl vinyl ketone (MVK) catalyzed by *N*-methylprolinol was investigated using density functional theory (DFT) method. The overall reaction includes two steps: C–C bond formation and hydrogen migration. In the presence of water, the hydrogen migration occurs *via* a six-membered ring transition state and the corresponding energy barrier decreases dramatically, and therefore the RDS is the C–C bond formation step. The calculations indicate that the C–C bond formation step controls the stereochemistry of the reaction. In this step, the hydrogen bonding induces the direction of the attack of enamine to aldehyde from the –OH group side of *N*-methylprolinol. The energy-favored transition states are mainly stabilized by hydrogen bonding, while the chirality of the products is affected by the hydrogen bonding and the steric hindrance. The calculations correctly reproduce the major product in (*R*)-configuration, which is consistent with the experimental observation.

Introduction

The Morita–Baylis–Hillman reaction is one of the most versatile C–C bond formation reactions in modern organic synthesis. Baylis and Hillman first reported Baylis–Hillman reaction of acetaldehyde with ethyl acrylate and acrylonitrile in the presence of catalytic amounts of 1,4-diazabicyclo [2,2,2] octane (DABCO).[1] Generally, the reaction involves the coupling of an unsaturated carbonyl compound with aldehyde to produce α-methylene-β-hydroxy carbonyl compound in one-step[2] (Scheme 1). Due to its advantages, such as atomic economy, nonmetal catalysis, mild reaction conditions and compatibility with multiple functional groups, *etc.*,[2a,3] the MBH reaction has attracted considerable attention in the past decade in synthesis chemistry.

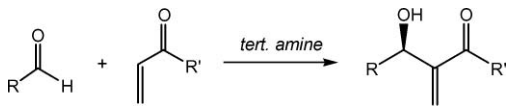

Scheme 1 The typical MBH reaction.

The development of an efficient MBH reaction is among the most challenging themes in organic synthesis,[4] for the efficiency of the MBH reaction is often poor and long-sustained reaction time is usually needed (at least 1 week, sometimes even 1 month). To overcome these disadvantages, many catalysts have been developed and introduced into this kind of reaction, such as substituted DABCOs, pyrrolizidine, tertiary amine, tributyl phosphine, *etc.*[5] Among numerous novel catalysts, the chiral catalysts with bifunctional groups (chiral amine, or phosphine catalysts bearing an alcohol function[6]) are found to be the most effective.[6e–6f,7]

As one chiral bifunctional catalyst, prolinol has been developed in the field of asymmetric catalysis.[8,9] Krishna *et al.* reported that the MBH reaction between MVK and benzaldehyde catalyzed by *N*-methylprolinol afforded the corresponding product (*R*-configuration) in good yield (80%) with moderate to good enantioselectivity (78% *ee*) in the protic solvents, and the reaction time was only 40 h.[8] Experimental investigations proposed that the –OH group disposed on an amine catalyst might be responsible for the good catalytic performance of the bifunctional catalysts, for –OH group could stabilize the oxy anion intermediate through hydrogen bonding and exert a distinct effect on rate acceleration.[6g,6i]

For the reaction mechanism, the experimental evidences of a MBH reaction[10] were liable to support the reaction route in Scheme 2. The rate-determining step of the MBH reaction, however, is still in debate so far. In the widely employed Hill and Isaacs's mechanism, the C–C bond formation step (step 2) was considered as the RDS,[11] but recent experimental investigations

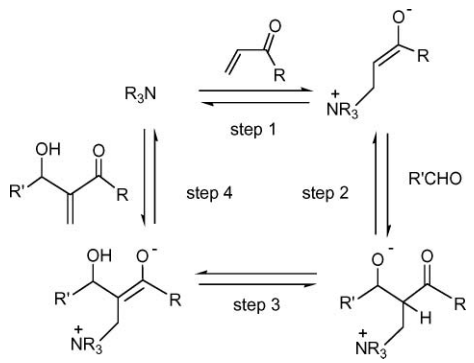

Scheme 2 The mechanism of the MBH reaction.

Key Laboratory of Green Chemistry and Technology, Ministry of Education, College of Chemistry, Sichuan University, Chengdu, Sichuan, 610064, China. E-mail: chwehu@mail.sc.cninfo.net, gchem@scu.edu.cn

† Electronic supplementary information (ESI) available: Computational methods, energies and geometries, AIM analysis, geometry evolution and charge transfer in C–C bond formation, energy profiles along different paths in the presence of water, complete paths *via si-syn*-OH-TS2, *re-anti*-OH-TS3. See DOI: 10.1039/c004932h

proposed that the hydrogen migration step (step 3) was the RDS instead of the C–C bond formation step.[12]

Theoretically, the related investigations on the MBH reaction based on quantum chemistry indicated that the reaction mechanism might be sensitive to the solvents. Sunoj and co-workers[13] proposed the detailed mechanism of the MBH reaction catalyzed by DABCO under aprotic conditions using *ab initio* and DFT methods. The RDS was identified as the intramolecular hydrogen migration step after the C–C bond formation step. Subsequently they demonstrated that the MBH reaction was favored in water solvent.[14] Recently, they extended their investigations onto aza-Morita–Baylis–Hillman reaction and suggested that the polar protic solvents facilitate this reaction.[15] Aggarwal, Harvey and co-workers[16] explored the mechanism of the MBH reaction between methyl acrylate and benzaldehyde catalyzed by a tertiary amine in the absence of protic species and in the presence of methanol. They identified the mechanism proposed by McQuade where in the absence of protic species the hydrogen migration was accomplished by addition of a second aldehyde to form a hemiacetal alkoxide. They also proposed that methanol acted as a shuttle to help hydrogen migration and made the energy barrier lower when methanol participated in the reaction. In their mechanism, the hydrogen migration step was the RDS.

Although great effort has been made to explain the mechanism of the MBH reaction, the detailed information at molecular level about the mechanism over the chiral bifunctional catalyst is much less known. In an attempt to gain a better understanding of the MBH reaction and to clarify how the chiral bifunctional catalyst accelerates the reaction rate, we used DFT method to investigate the detailed mechanism of the MBH reaction between MVK and aldehyde catalyzed by bifunctional catalyst *N*-methylprolinol. The origin of the stereoselectivity of the actual *N*-methylprolinol-catalyzed MBH reaction between MVK and benzaldehyde (Scheme 3) was also investigated in this paper.

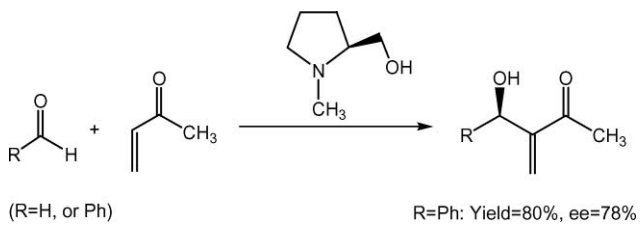

Scheme 3 The *N*-methylprolinol-catalyzed MBH reaction used in present simulation.

Computational details

Among the correlated functional theories, B3LYP performs well for organic reactions, such as for the nucleophilic reactions[19] and hydrogen bonding systems.[20] The previous investigation also indicated that B3LYP method can give reasonable structures and energies for the MBH reaction.[16] All stationary points on the potential energy surface (PES) were optimized using hybrid density functional B3LYP[17] method with the 6-311++G(d,p) basis set.[18] Zero-point vibrational energies (ZPVE) and basis-set superposition error (BSSE) corrections were also applied in relative energies. Vibrational frequencies were obtained at the same level, and the species were characterized as a minimum (no imaginary frequency) or a transition state (unique imaginary frequency). Intrinsic reaction coordinate (IRC) calculations were performed to further confirm that the optimized transition state correctly connects the relevant reactant and product. Considering the effect of the solvent, single-point B3LYP (PCM[21])/[6-311++G(d,p)] calculations were performed on the optimized structures. In the experiments the reaction was performed in mixed solvent (1,4-dioxane:water/1 : 1),[8] and therefore the PCM calculations were performed in 1,4-dioxane and water, respectively. The chemical bonding properties were analyzed following the concepts developed in the theory of atoms-in-molecules (AIM2000), which provides a clear definition of a chemical bond by means of a topology analysis of $\rho(r)$.[22] To obtain a further insight into the electroproperties along the reaction, natural bond orbital (NBO) analysis[23] at the B3LYP/6-311++G(d,p) level was performed. The electrophilicity analysis concerning the electrophilicity index ω[24] was also performed.

All calculations were carried out using the Gaussian 03 program.[25]

Results and discussion

Mechanism of reaction

Our calculations starts from the simulation on the MBH reaction between MVK and formaldehyde catalyzed by *N*-methylprolinol. Fig. 1 shows the calculated PES in 1,4-dioxane at the B3LYP/6-311++G(d,p) level. PCM energies in water are also presented in Fig. 1. The results in the gas-phase are consistent with that in 1,4-dioxane. The relative energies in the gas-phase are listed for supplementary.

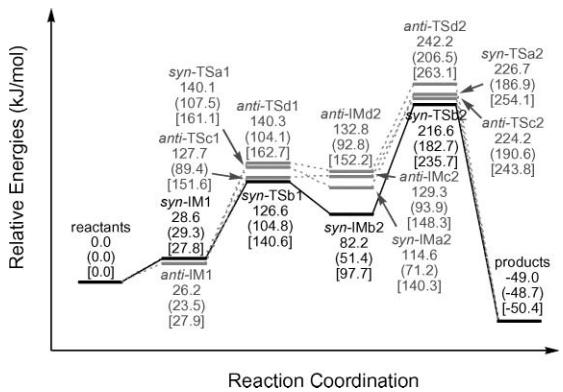

Fig. 1 PCM energies (in kJ mol^{-1}) in 1,4-dioxane for various intermediates and transition states calculated at the B3LYP/6-311++G(d,p) level. PCM energies (in kJ mol^{-1}) in water are listed in parentheses. The relative energies (in kJ mol^{-1}) in the gas-phase are listed in square brackets.

Our calculations indicate that the overall reaction is in general composed of two steps as follows: (1) The C–C bond formation step: *N*-methylprolinol coordinates to MVK, generating an enamine intermediate (IM1) to attack formaldehyde producing a zwitterionic intermediate (IM2) *via* TS1. (2) The hydrogen migration step: the hydrogen migrates from enamine to formaldehyde *via* TS2 followed by the expulsion of *N*-methylprolinol to release the MBH product with the recovery of the catalyst. Here, four paths similar in mechanism and energies are obtained. For the major part of path *b* is the most kinetically and thermodynamically favored in

1,4-dioxane or water, it was chosen to illustrate the mechanism of the MBH reaction. The path *b* and the corresponding optimized structures are given in Fig. 2.

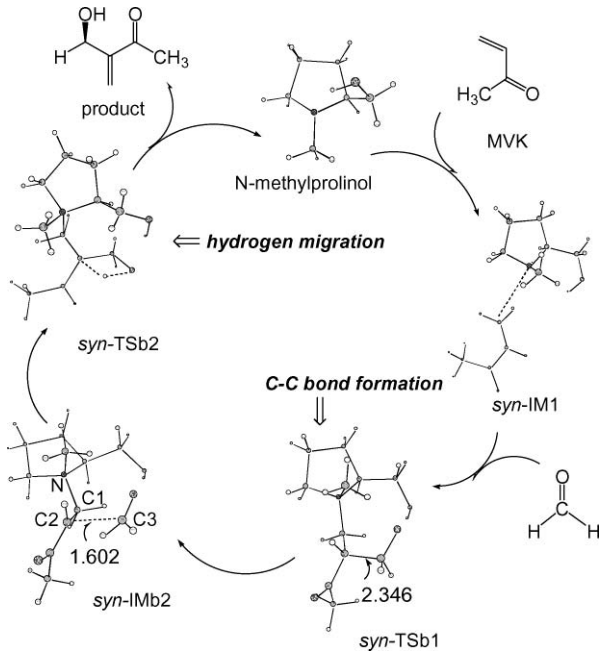

Fig. 2 The optimized structures along path *b* (bond length in Å).

C–C bond formation step

As shown in Fig. 2, the predicted reaction starts from the formation of enamine intermediate *syn*-IM1 in path *b*. From *syn*-IM1, the C–C bond formation process occurs *via* the transition state *syn*-TSb1, corresponding to the attack of enamine to formaldehyde from the –OH group side of *N*-methylprolinol. Next, the corresponding intermediate *syn*-IMb2 forms. As shown in Fig. 2, the bond length between enamine and formaldehyde in *syn*-TSb1 is 2.346 Å. The C–C bond distance in *syn*-IMb2 shortens to 1.602 Å.

With the analysis of NBO[23] and the electrophilicity index ω,[24] it is concluded that after the *syn*-enamine attacks formaldehyde, the charge transfers from N atom of *N*-methylprolinol to MVK. The increasing charge on MVK makes the interaction between MVK and *N*-methylprolinol greater and the structure of *syn*-TSb1 becomes more compact, as compared to the structure in *syn*-enamine. On the other hand, the charge accumulated on C2 atom makes MVK more nucleophilic and then enhances the interaction between MVK and formaldehyde (details in the ESI†).

Hydrogen migration step

From *syn*-IMb2, the hydrogen migration of enamine to formaldehyde occurs. The transition state concerning direct hydrogen migration (*syn*-TSb2) in path *b* is depicted in Fig. 3.

As shown in Fig. 3, the distances of O1–H2, C2–H2 bond are 1.384 Å and 1.317 Å, respectively. The corresponding bond angle of C2–H2–O1 is 113°. The above results suggest that the direct hydrogen migration occurs *via* a four-membered ring transition state (involving C2, C3, O1 and H2 atom). The relative

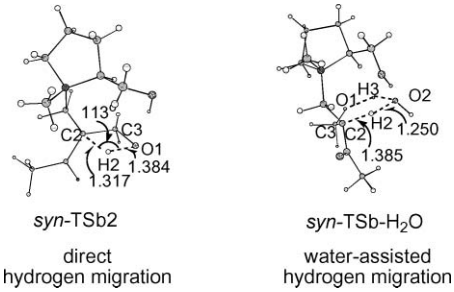

Fig. 3 The optimized transition states concerning direct hydrogen migration and the water-assisted hydrogen migration. (bond length in Å).

energy of direct hydrogen migration in path *b* is calculated to be 216.6 kJ mol^{-1} in 1,4-dioxane (or 182.7 kJ mol^{-1} in water), which is rather high for mild condition in experiments.

On the other hand, numerous experimental studies[26] suggested that the rate of the MBH reaction is increased in the presence of water or other polar protic solvents. The previous theoretical investigations[13–16] indicated that water might facilitate the MBH reaction. Here, one water molecule assisted-reaction model was employed to establish the role of protic species on reaction mechanism. The energy profiles concerning direct hydrogen migration mechanism and one water-assisted hydrogen migration mechanism along path *b* at the B3LYP/6-311++G(d,p) level are shown in Fig. 4. The optimized structure of one water-assisted hydrogen migration transition state (*syn*-TSb-H_2O) is depicted in Fig. 3.

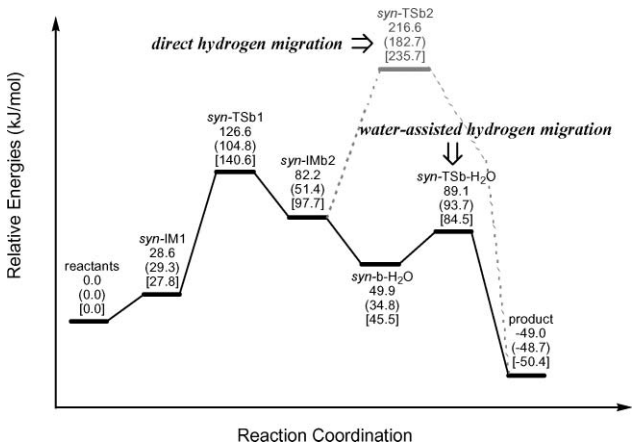

Fig. 4 PCM energies (in kJ mol^{-1}) in 1,4-dioxane for various intermediates and transition states calculated at the B3LYP/6-311++G(d,p) level. PCM energies (in kJ mol^{-1}) in water are listed in parentheses. The relative energies (in kJ mol^{-1}) in the gas-phase are listed in square brackets.

As shown in Fig. 3, the hydrogen migration involving a water molecule occurs *via* a six-membered ring (consisted of C2, C3, O1, O2, H2 and H3 atom) transition state. The whole hydrogen migration process includes the migration of H2 to O2 and H3 to O1. The net result of this one-step two proton-transfer process generates the product, accompanied by the formation of another water molecule. As proposed by Yu's group, the water-catalyzed [1,2]-hydrogen shift adopts a proton-transport catalysis strategy in the Au(I)-catalyzed tandem reaction system.[27] It is noted that in previous investigations, even though more than one water molecule were employed, the similar situation occurs.[14–16] In the present

system, the water molecule acts as the analogous proton shuttle to transport a proton from C2 to O1.

As shown in Fig. 4, the relative energies of *syn*-TSb-H_2O is 89.1 kJ mol^{-1} in 1,4-dioxane (or 93.7 kJ mol^{-1} in water), much lower than that of *syn*-TSb2 along the direct hydrogen migration path. The result indicates that water molecule facilitates the reaction through relaying proton *via* the six-membered ring hydrogen migration transition state, as compared to the hydrogen migration without water molecule involved. The reaction profiles of other paths are similar with that of path *b* (see ESI†). The previous investigation concerning the role of water in the MBH reaction proposed that the remarkable decrease in relative energy could be ascribed to the alleviation of ring strain in hydrogen migration transition state upon changing from a four- to a six-membered ring transition state and the specific hydrogen bonding interaction in six-membered ring transition state.[14] We also considered the possibility in which water molecule participates in the first step (from IM1 to IM2), but the calculations failed to locate the corresponding structures. These results are consistent with the previous assumptions proposed by Sunoj, Aggarwal and Harvey.[14–16] Furthermore, as shown in Fig. 4, when water participates in the reaction, the RDS can be identified as the C–C bond formation step *via syn*-TSb1.

It should be emphasized that the bulk effect of the each solvent by PCM calculations does not change significantly the positions of the minima but reduces the relative energies of potential energy surface (PES). Especially in water, the energies of the PES are much lower than these in the gas-phase or in 1,4-dioxane (relative energies in the gas-phase are listed in the ESI†). Even if the bulk effect is only considered, the reaction might be thermodynamically favored in each solvent. On the other hand, it is found that water might participate in the hydrogen migration and then remarkably reduce the energy barrier of this step. Hence, as compared to 1,4-dioxane, water might exert double-effect (bulk effect and hydrogen shuttle) on the reaction mechanism.

Stereochemistry of reaction

After we got the mechanism of the MBH reaction, we turned our attention to the stereochemistry of this reaction. Normally, the conformation of enamine intermediate (IM1) is crucial for the enantiomeric formation of the desired products, the binding mode of the catalyst and the substrate was first explored to establish the conformation of enamine IM1.

Binding mode of the catalyst with the substrate

For the virtue of the potential chirality of *N*-methylprolinol, MVK can be alternatively positioned in *syn* or *anti* conformation with respect to *N*-methylprolinol in IM1. Therefore two enamine intermediates (*syn*-IM1 and *anti*-IM1) are located as the energy minima. The optimized structures are given in Fig. 5. The distances between the N atom of *N*-methylprolinol and C1 atom of MVK are calculated to be 3.894 Å in *syn*-IM1 and 4.214 Å in *anti*-IM1, respectively. Both in 1,4-dioxane and water, PCM calculations place IM1 *ca.* 29 kJ mol^{-1} higher than the separated *N*-methylprolinol and MVK in relative energies. The above results suggest that in enamine intermediate IM1, MVK loosely interacts with *N*-methylprolinol.

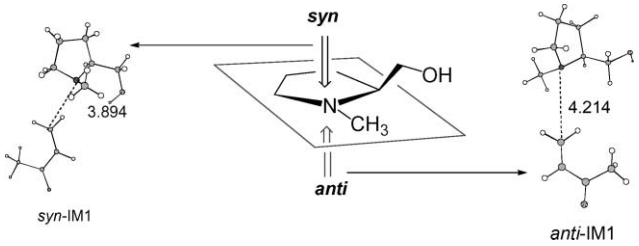

Fig. 5 The optimized structures of enamine intermediates.

Attacking direction of enamine to aldehyde

As mentioned above, in the presence of water, the C–C bond formation step is the RDS. During this step, the attacking direction plays an important role to determine the conformation of final product. Therefore, it can be deduced that this step is not only the RDS but also the stereo-controlling step (SCS) in the presence of water. In order to establish the attacking direction of the MBH reaction more clearly, formaldehyde is used in this section for its simplest structure.

Since enamine intermediates could attack formaldehyde from two faces, four distinct transition states result, marked as *syn*-TSa1, *syn*-TSb1, *anti*-TSc1 and *anti*-TSd1, respectively. *syn*-TSa1, *anti*-TSd1 correspond to enamine intermediates attack formaldehyde from –CH_3 group side and *syn*-TSb1, *anti*-TSc1 correspond to enamine intermediates attack formaldehyde from –OH group side. The optimized structures of the C–C bond formation transition states along different paths are given in Fig. 6.

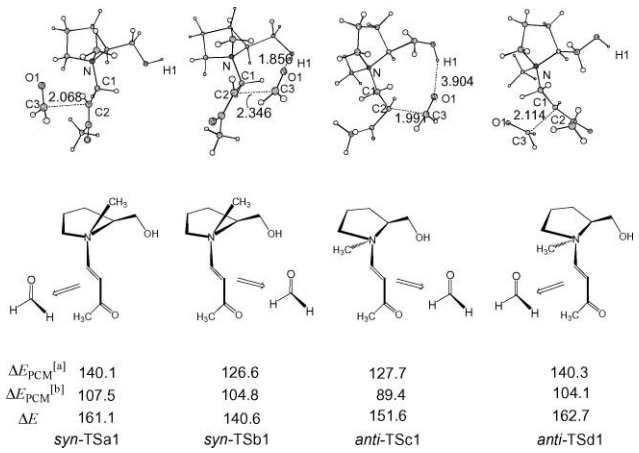

Fig. 6 The optimized structures of the C–C bond formation transition states along different paths. (bond length in Å) Relative energies (in kJ mol^{-1}) in 1,4-dioxane[a], water[b] and in the gas-phase for various transition states calculated at the B3LYP/6-311++G(d,p) level.

In *syn*-TSb1 and *anti*-TSc1, the attack of enamine takes place from the –OH group side of *N*-methylprolinol, while in *syn*-TSa1 and *anti*-TSd1, the attack of enamine occurs from the opposite side. Our calculations indicate that the transition states (*syn*-TSb1, *anti*-TSc1) along the path *b* and path *c*, corresponding to the attack of enamine from the –OH group side of *N*-methylprolinol, are kinetically favored by *ca.* 15 kJ mol^{-1} in 1,4-dioxane, as compared to those along the path *a* and path *d* (*syn*-TSa1, *anti*-TSd1).

Table 1 The O1···H1 distance between the –OH group of *N*-methylprolinol and the O atom of carbonyl in formaldehyde of TS1s. (Å)

	syn-TSa1	*syn*-TSb1	*anti*-TSc1	*anti*-TSd1
O1···H1 Distance	6.794	1.856	3.904	7.051

It should be noted that along path *b* and path *c*, when enamine attacks formaldehyde from the –OH group side of *N*-methylprolinol, this attack makes O atom of carbonyl in formaldehyde (O1) close to the –OH group of *N*-methylprolinol. Especially in *syn*-TSb1 along path *b*, the O1…H1 distance is only 1.856 Å. AIM analysis[22] indicates that the calculated Laplacian $L(r)$ at the bond critical point between H1 and O1 in *syn*-TSb1 is –0.026 au, showing the formation of hydrogen-bond between H1 and O1 (details in ESI†). Similarly, the hydrogen bonding interaction exists in *anti*-TSc1, suggested by the O1···H1 distance of 3.904 Å and its Laplacian value of –0.017 au. As compared to *syn*-TSb1 and *anti*-TSc1 shown in Fig. 6, hydrogen bonding interaction between H1 and O1 unlikely exists in *syn*-TSa1 and *anti*-TSd1, suggested by the correspond O1…H1 distance listed in Table 1. Besides, there is no significant difference in structural distortion in the four structures of TS1s. For the hydrogen bonding interaction stabilizes *syn*-TSb1 and *anti*-TSc1, the relative energies in 1,4-dioxane are *ca.* 15 kJ mol^{-1} lower than that of *syn*-TSa1 and *anti*-TSd1.

As shown in Fig. 6, however, the PCM calculations in water might underestimate the hydrogen bonding interaction in *syn*-TSb1, for the relative energy of *syn*-TSb1 is comparable with that in *anti*-TSc1 in water.

Stereoselectivities of products

Although the above simulations identified four distinct attacking modes, formaldehyde system just generates the racemic mixtures. Actually, benzaldehyde is usually used as the actual substrate in experiments. Krishna *et al.* reported that the MBH reaction between MVK and benzaldehyde catalyzed by *N*-methylprolinol can give the relatively higher stereoselectivities (78%) (in Scheme 3).[8] On the basis of the experimental data, the actual reaction system between MVK and benzaldehyde catalyzed by *N*-methylprolinol was chosen to investigate the stereoselectivities of the products.

Because enamine intermediate can attack benzaldehyde from *re* or *si* face of benzaldehyde and leads to the (*S*)- or (*R*)-product. Eight diastereomeric transition states were located. The sketch map of the formation of the diastereoisomers are presented in Scheme 4.

The optimized structures of the eight transition states are provided in Fig. 7. The configuration of products and the PCM energies of solvation at the B3LYP/6-311++G(d,p) level are summarized in Table 2. Among the eight diastereomers, four isomers correspond to the attack of enamine from the –OH group side of *N*-methylprolinol: *re-syn*-OH-TS1 to *si-anti*-OH-TS4 (prefix *re-* presents the attack of enamine to *re* face of benzaldehyde, and prefix *si-* to *si* face). In contrast, four other isomers correspond to the attack of enamine to benzaldehyde from –CH_3 group side: *si-syn*-CH_3-TS1 to *re-anti*-CH_3-TS4.

From Table 2 and Fig. 7, it is found that a noticeable energy distinction exists among the eight transition states in 1,4-dioxane.

Table 2 Relative energies (in kJ mol^{-1}) of the optimized structures at the B3LYP/6-311++G(d,p) level

Structures	Product Configuration	τ (%)[a]	ΔE_{PCM}[b]	ΔE_{PCM}[c]	ΔE
re-syn-OH-TS1	*S*	0.8	157.3	133.8	168.5
si-syn-OH-TS2	*R*	87.1	145.7	126.8	154.0
re-anti-OH-TS3	*S*	5.8	152.4	135.8	159.0
si-anti-OH-TS4	*R*	4.6	153.0	137.6	160.0
si-syn-CH_3-TS1	*R*	—	170.9	144.6	182.4
re-syn-CH_3-TS2	*S*	1.7	155.5	117.0	177.1
si-anti-CH_3-TS3	*R*	—	196.8	163.4	213.2
re-anti-CH_3-TS4	*S*	—	172.4	135.8	189.8

[a] τ: Occupied probability based on Boltzmann distribution in 1,4-dioxane, $\tau = N_i^*/N = [g_i\exp(-\varepsilon_i/kT)]/[\sum g_i\exp(-\varepsilon_i/kT)]$ (T = 298.15 K). ee = $(\sum\tau^R - \sum\tau^S)/\sum(\tau^R + \tau^S)$ = 83.4%. [b] Single-point B3LYP (PCM, 1,4-dioxane)/[6-311++G(d,p)] calculations. [c] Single-point B3LYP (PCM, H_2O)/[6-311++G(d,p)] calculations.

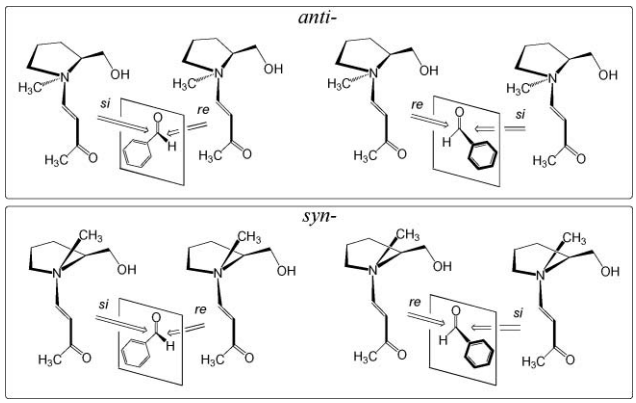

Scheme 4 The sketch map of the formation of the diastereoisomers.

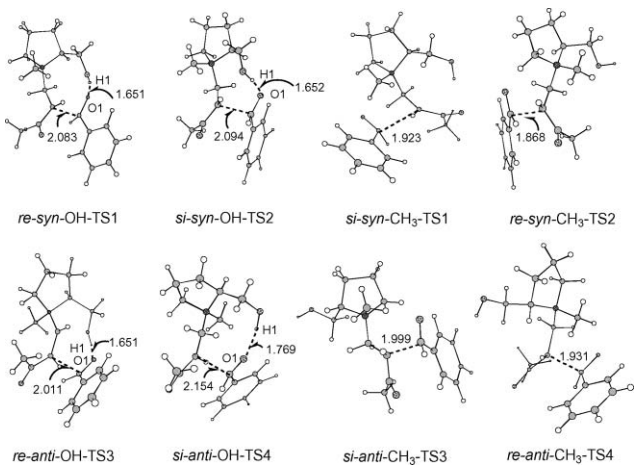

Fig. 7 Optimized structures of the eight possible transition states of the C–C bond formation step. (bond length in Å).

The four TSs in which enamine attacks benzaldehyde from –OH group side are more stable than their analogs from –CH_3 group side. In OH-TSs, the short distance of O1…H1 between the –OH group on *N*-methylprolinol and the O atom of carbonyl in benzaldehyde varies from 1.651 to 1.769 Å, listed in Table 3. AIM analysis indicates that the calculated Laplacian value is –0.031~–0.035 au at the bond critical point between H1 and O1

Table 3 The Laplacian value (au) and the O1 · · · H1 distance (Å) between the –OH group of *N*-methylprolinol and the O atom of carbonyl in benzaldehyde of OH-TSs

	re-syn-OH-TS1	*si-syn*-OH-TS2
O1 · · · H1 Distance	1.651	1.652
L(*r*)	–0.035	–0.034
	re-anti-OH-TS3	*si-anti*-OH-TS4
O1 · · · H1 Distance	1.651	1.769
L(*r*)	–0.035	–0.031

in OH-TSs, showing the formation of O1…H1 hydrogen bonding between the –OH group and the O atom in benzaldehyde. In contrast, as compared to OH-TSs, the attacking directions of enamine to benzaldehyde make the –OH group far from the carbonyl group of benzaldehyde in CH_3-TSs. Hydrogen bonding interaction between H1 and O1 unlikely exists in the CH_3-TSs. Combined with the above discussions, it is concluded that the energies of OH-TSs are lower than that of CH_3-TSs due to the hydrogen bonding. For the present actual system, the calculations indicate that the –OH group of *N*-methylprolinol might induce the direction of the attack of enamine from the –OH group side of *N*-methylprolinol to MVK in term of hydrogen bonding interaction between –OH group and the O atom of carbonyl in benzaldehyde. These results are compatible with those in formaldehyde system.

Compared with the calculated PCM energies in 1,4-dioxane of the four OH-TSs shown in Table 2, the two lowest-energy transition states *si-syn*-OH-TS2 and *re-anti*-OH-TS3 for *si* and *re* attack to benzaldehyde correspond to (*R*)- and (*S*)-product respectively. The nucleophilic addition to *si* face of benzaldehyde is preferred by 6.7 kJ mol^{-1} in relative energies. Based on the absolute rate theory, the energy difference predicts that the (*R*)-configuration might be the predominant product in the reaction. This is consistent with the experimental observation. (The complete paths *via* the two competitive TSs, are presented in the ESI† and the overall reaction profile is found to be qualitatively similar to that of the model reaction.) The kinetically preferred transition state in the gas-phase also leads to the major product in (*R*)-configuration.

According to the Boltzmann distribution, PCM energies in 1,4-dioxane (in Table 2) predicts the selectivity for the corresponding (*R*)-product should be 87.1% (corresponding to 83.4% *ee*), which is slightly overestimated as compared to the experimental value (78% *ee*). In the lower-energy *si-syn*-OH-TS2, the phenyl ring is situated *anti* to the terminal double bond of MVK and becomes less-hindered. In *re-anti*-OH-TS3, the phenyl ring is situated *syn* to the terminal double bond within a repulsive steric interaction. The above results imply that the energy gap between *si-syn*-OH-TS2 and *re-anti*-OH-TS3 is generated from the steric hindrance between the phenyl ring of benzaldehyde and the terminal double bond of MVK.

The calculations indicate that in 1,4-dioxane the diastereomeric transition states are mainly stabilized by hydrogen bonding, while the chirality of the products is controlled by the hydrogen bonding and the steric hindrance. The kinetically preferred transition state *si-syn*-OH-TS2 would lead to the major product in (*R*)-configuration.

It should be noted that the PCM calculations in water predict the major product in (*S*)-configuration with 97.8% *ee*, according to the Boltzmann distribution. The prediction is different to that in 1,4-dioxane and this means the present reaction system is sensitive to solvent. Since there is no experimental evidence, it is difficult to evaluate quantitatively the validity of the theoretical prediction. Meanwhile, although the PCM model is expected to give a qualitative indication of bulk effect of solvents, it is unlikely to be able to reliably predict the effect of surrounding these polar systems with water, such as hydrogen bonding is not accounted for.[28] Therefore, PCM model may not be very suitable for evaluating the bulk effect of water on the stereoselectivity in the present system.

Combined with the present theoretical results and experimental evidences, it is suggested that the reaction should be significantly sensitive to the solvent. In the present mixed solvent, 1,4-dioxane might guarantee the stereoselectivity and water accelerate the reaction rate, which might be the reason why the actual reactions were carried out in the mixed solvent.

Conclusions

The mechanism and the stereoselectivity of the Morita–Baylis–Hillman reaction catalyzed by *N*-methylprolinol have been investigated using density functional theory (DFT) method at the B3LYP/6-311++G(d,p) level. The effect of the chiral bifunctional catalyst *N*-methylprolinol on the mechanism and the selectivities are also interpreted. The major conclusions are listed as the following:

The catalytic cycle may include two steps in general: C–C bond formation and hydrogen migration. In the presence of water, the hydrogen migration occurs *via* a six-membered ring transition state and the corresponding energy barrier decreases dramatically. The RDS is the C–C bond formation step in the presence of water.

The C–C bond formation step controls the stereochemistry of the reaction. In this step, the hydrogen bonding induces the direction of the attack of enamine intermediates to aldehyde from the –OH group side of *N*-methylprolinol. The diastereomeric transition states are mainly stabilized by hydrogen bonding and the chirality of the products is affected by the hydrogen bonding and the steric hindrance. The major product in (*R*)-configuration reproduced theoretically is consistent with the experimental observation.

Acknowledgements

The authors are gratefully for the financial support provided by NNSF (Nos. 20732003 and 20772085) and PCSIRT (No.IRT0846) of China, Specialized Research Fund for the Doctoral Program of Higher Education (No.200806101007).

References

1 (*a*) A. B. Baylis and M. E. D. Hillman, German Patent 2155113, 1972; A. B. Baylis and M. E. D. Hillman, *Chem. Abstr.*, 1972, **77**, 34174q; (*b*) M. E. D. Hillman and A. B. Baylis, US Patent 3743669, 1973.
2 (*a*) D. Basavaiah, A. J. Rao and T. Satyanarayana, *Chem. Rev.*, 2003, **103**, 811; (*b*) M. J. Gaunt and C. C. C. Johansson, *Chem. Rev.*, 2007, **107**, 5596; (*c*) M. Shi, L. Chen and C. Li, *J. Am. Chem. Soc.*, 2005, **127**, 3790; (*d*) G. Masson, C. Housseman and J. Zhu, *Angew. Chem., Int. Ed.*, 2007, **46**, 4614.
3 (*a*) S. France, D. J. Guerin, S. J. Miller and T. Lectka, *Chem. Rev.*, 2003, **103**, 2985; (*b*) V. Declerck, J. Martinez and F. Lamaty, *Chem. Rev.*, 2009, **109**, 1.

4 (*a*) D. Basavaiah, P. D. Rao and R. S. Hyma, *Tetrahedron*, 1996, **52**, 8001; (*b*) D. Basavaiah, K. V. Rao and R. J. Reddy, *Chem. Soc. Rev.*, 2007, **36**, 1581; (*c*) E. Tarsis, A. Gromova, D. Lim, G. Zhou and D. M. Coltart, *Org. Lett.*, 2008, **10**, 4819; (*d*) A. Bugarin and B. T. Connell, *J. Org. Chem.*, 2009, **74**, 4638.

5 (*a*) M. Shi, C. Li and J. Jiang, *Tetrahedron*, 2003, **59**, 1181; (*b*) L. J. Brzezinski, S. Rafel and J. W. Leahy, *J. Am. Chem. Soc.*, 1997, **119**, 4317.

6 (*a*) M. Shi and J. Jiang, *Tetrahedron: Asymmetry*, 2002, **13**, 1941; (*b*) F. Giacalone, M. Gruttadauria, A. M. Marculescu, F. D'Anna and R. Noto, *Catal. Commun.*, 2008, **9**, 1477; (*c*) N. Abermil, G. Masson and J. Zhu, *J. Am. Chem. Soc.*, 2008, **130**, 12596; (*d*) L. He, T. Jian and S. Ye, *J. Org. Chem.*, 2007, **72**, 7466; (*e*) A. Berkessel, K. Roland and J. M. Neudörfl, *Org. Lett.*, 2006, **8**, 4195; (*f*) J. Wang, H. Li, X. Yu, L. Zu and W. Wang, *Org. Lett.*, 2005, **7**, 4293; (*g*) S. E. Drewes, S. D. Freese, N. D. Emslie and G. H. P. Roos, *Synth. Commun.*, 1988, **18**, 1565; (*h*) K. Ito, K. Nishida and T. Gotanda, *Tetrahedron Lett.*, 2007, **48**, 6147; (*i*) I. E. Markó, P. R. Giles and N. J. Hindley, *Tetrahedron*, 1997, **53**, 1015; (*j*) M. Shi, J. Jiang and C. Li, *Tetrahedron Lett.*, 2002, **43**, 127.

7 (*a*) A. Nakano, K. Takahashi, J. Ishihara and S. Hatakeyama, *Org. Lett.*, 2006, **8**, 5357; (*b*) A. Nakano, S. Kawahara, S. Akamatsu, K. Morokuma, M. Nakatani, Y. Iwabuchi, K. Takahashi, J. Ishihara and S. Hatakeyama, *Tetrahedron*, 2006, **62**, 381.

8 P. R. Krishna, V. Kannan and P. V. N. Reddy, *Adv. Synth. Catal.*, 2004, **346**, 603.

9 (*a*) P. J. Chua, B. Tan, X. Zeng and G. Zhong, *Bioorg. Med. Chem. Lett.*, 2009, **19**, 3915; (*b*) S. Goushi, K. Funabiki, M. Ohta, K. Hatano and M. Matsui, *Tetrahedron*, 2007, **63**, 4061; (*c*) Y. Li, X. Liu, Y. Yang and G. Zhao, *J. Org. Chem.*, 2007, **72**, 288; (*d*) A. Lattanzi, *Org. Lett.*, 2005, **7**, 2579.

10 (*a*) M. E. Krafft, T. F. N. Haxell, K. A. Seibert and K. A. Abboud, *J. Am. Chem. Soc.*, 2006, **128**, 4174; (*b*) L. S. Santos, C. H. Pavam, W. P. Almeida, F. Coelho and M. N. Eberlin, *Angew. Chem., Int. Ed.*, 2004, **43**, 4330; (*c*) G. W. Amarante, H. M. S. Milagre, B. G. Vaz, B. R. V. Ferreira, M. N. Eberlin and F. Coelho, *J. Org. Chem.*, 2009, **74**, 3031; (*d*) V. K. Aggarwal, S. Y. Fulford and G. C. Lloyd-Jones, *Angew. Chem., Int. Ed.*, 2005, **44**, 1706.

11 J. S. Hill and N. S. Isaacs, *J. Phys. Org. Chem.*, 1990, **3**, 285.

12 (*a*) K. E. Price, S. J. Broadwater, H. M. Jung and D. T. McQuade, *Org. Lett.*, 2005, **7**, 147; (*b*) K. E. Price, S. J. Broadwater, B. J. Walker and D. T. McQuade, *J. Org. Chem.*, 2005, **70**, 3980.

13 D. Roy and R. B. Sunoj, *Org. Lett.*, 2007, **9**, 4873.

14 D. Roy and R. B. Sunoj, *Chem.–Eur. J.*, 2008, **14**, 10530.

15 D. Roy, C. Patel and R. B. Sunoj, *J. Org. Chem.*, 2009, **74**, 6936.

16 R. Robiette, V. K. Aggarwal and J. N. Harvey, *J. Am. Chem. Soc.*, 2007, **129**, 15513.

17 (*a*) A. D. Becke, *J. Chem. Phys.*, 1993, **98**, 5648; (*b*) B. Miehlich, A. Savin, H. Stoll and H. Preuss, *Chem. Phys. Lett.*, 1989, **157**, 200; (*c*) R. Ditchfield, W. J. Hehre and J. A. Pople, *J. Chem. Phys.*, 1971, **54**, 724.

18 (*a*) W. J. Hehre, R. Ditchfield and J. A. Pople, *J. Chem. Phys.*, 1972, **56**, 2257; (*b*) P. C. Hariharan and J. A. Pople, *Mol. Phys.*, 1974, **27**, 209; (*c*) M. S. Gordon, *Chem. Phys. Lett.*, 1980, **76**, 163; (*d*) P. C. Hariharan and J. A. Pople, *Theor. Chim. Acta*, 1973, **28**, 213.

19 (*a*) A. P. Bento, M. Solá and F. M. Bickelhaupt, *J. Comput. Chem.*, 2005, **26**, 1497; (*b*) M. Swart, M. Solá and F. M. Bickelhaupt, *J. Comput. Chem.*, 2007, **28**, 1551; (*c*) X. Xu and W. A. Goddard III, *J. Phys. Chem. A*, 2004, **108**, 8495; (*d*) J. M. Gonzales, W. D. Allen and H. F. Schaefer III, *J. Phys. Chem. A*, 2005, **109**, 10613; (*e*) Y. Zhao and D. G. Truhlar, *Acc. Chem. Res.*, 2008, **41**, 157; (*f*) V. A. Guner, K. S. Khuong and K. N. Houk, *J. Phys. Chem. A*, 2004, **108**, 2959; (*g*) G. T. de Jong and F. M. Bickelhaupt,, *J. Phys. Chem. A*, 2005, **109**, 9685.

20 (*a*) V. S. Bryantsev, M. S. Diallo, A. C. T. van Duin and W. A. Goddard III, *J. Chem. Theory Comput.*, 2009, **5**, 1016; (*b*) L. Rao, H. Ke, G. Fu, X. Xu and Y. Yan, *J. Chem. Theory Comput.*, 2009, **5**, 86; (*c*) C. Lee, W. Yang and R. G. Parr, *Phys. Rev. B: Condens. Matter*, 1988, **37**, 785; (*d*) A. D. Becke, *Phys. Rev. A: At., Mol., Opt. Phys.*, 1988, **38**, 3098; (*e*) A. D. Becke, *J. Chem. Phys.*, 1993, **98**, 5648.

21 M. Cossi, V. Barone, B. Mennucci and J. Tomasi, *Chem. Phys. Lett.*, 1998, **286**, 253.

22 R. F. W. Bader *Atoms in Molecules. A Quantum Theory*, Clarendon Press, Oxford, 1990. For computer programs, see: Biegler-König, F. W.; Schönbohm, AIM2000. The program can be downloaded at http://www.aim2000.de/.

23 (*a*) J. Blaudeau, M. P. McGrath, L. A. Curtiss and L. Radom, *J. Chem. Phys.*, 1997, **107**, 5016; (*b*) M. M. Francl, W. J. Pietro, W. J. Hehre, J. S. Binkley, D. J. DeFrees, J. A. Pople and M. S. Gordon, *J. Chem. Phys.*, 1982, **77**, 3654.

24 R. G. Parr, L. v. Szentpály and S. Liu, *J. Am. Chem. Soc.*, 1999, **121**, 1922; the concept of electrophilicity index ω have been employed to gain a further interpretation of the entire reaction process.

25 M. J. Frisch, G. W. Trucks, H. B. Schlegel, G. E. Scuseria, M. A. Robb, J. R. Cheeseman, J. A. Jr. Montgomery, T. Vreven, K. N. Kudin, J. C. Burant, J. M. Millam, S. S. Iyengar, J. Tomasi, V. Barone, B. Mennucci, M. Cossi, G. Scalmani, N. Rega, G. A. Petersson, H. Nakatsuji, M. Hada, M. Ehara, K. Toyota, R. Fukuda, J. Hasegawa, M. Ishida, T. Nakajima, Y. Honda, O. Kitao, H. Nakai, M. Klene, X. Li, J. E. Knox, H. P. Hratchian, J. B. Cross, V. Bakken, C. Adamo, J. Jaramillo, R. Gomperts, R. E. Stratmann, O. Yazyev, A. J. Austin, R. Cammi, C. Pomelli, J. W. Ochterski, P. Y. Ayala, K. Morokuma, G. A. Voth, P. Salvador, J. J. Dannenberg, V. G. Zakrzewski, S. Dapprich, A. D. Daniels, M. C. Strain, O. Farkas, D. K. Malick, A. D. Rabuck, K. Raghavachari, J. B. Foresman, J. V. Ortiz, Q. Cui, A. G. Baboul, S. Clifford, J. Cioslowski, B. B. Stefanov, G. Liu, A. Liashenko, P. Piskorz, I. Komaromi, R. L. Martin, D. J. Fox, T. Keith, M. A. Al-Laham, C. Y. Peng, A. Nanayakkara, M. Challacombe, P. M. W. Gill, B. Johnson, W. Chen, M. W. Wong, C. Gonzalez and J. A. Pople, *Gaussian 03, B05*Gaussian, Inc.: Wallingford, CT, 2003.

26 (*a*) J. Cai, Z. Zhou, G. Zhao and C. Tang, *Org. Lett.*, 2002, **4**, 4723; (*b*) C. Faltin, E. M. Fleming and S. J. Connon, *J. Org. Chem.*, 2004, **69**, 6496; (*c*) V. K. Aggarwal, D. K. Dean, A. Mereu and R. Williams, *J. Org. Chem.*, 2002, **67**, 510; (*d*) S. Luo, B. Zhang, J. He, A. Janczuk, P. G. Wang and J. Cheng, *Tetrahedron Lett.*, 2002, **43**, 7369; (*e*) C. Yu, B. Liu and L. Hu, *J. Org. Chem.*, 2001, **66**, 5413.

27 F. Shi, X. Li, Y. Xia, L. Zhang and Z. Yu, *J. Am. Chem. Soc.*, 2007, **129**, 15503.

28 J. Kaminský and F. Jensen, *J. Chem. Theory Comput.*, 2007, **3**, 1774.